ingegneria sismica
International Journal of Earthquake Engineering
Anno XLIII - Num. 1 - 2026

Comparison of the Inheritance of Modern Lingnan Landscape Painting and Western Landscape Painting Techniques Based on Knowledge Mapping

Bing Wu[1,*]

[1] School of Fine Arts, Zhaoqing University, Zhaoqing, Guangdong, 526061, China

SUMMARY: *In order to analyze the similarities and differences in the technical inheritance of modern Lingnan landscape paintings and Western landscape paintings, this paper proposes a knowledge graph construction method oriented to the multimodal attribute information of paintings. The EIEA model is adopted for multimodal entity alignment, and the unimodal-based entity embedding is obtained through multiple pre-trained models. An enhanced entity representation module is developed to mine the interaction information between paired entity nodes. The ERNIE model is utilized to complete the relationship extraction and knowledge fusion tasks to construct a multimodal knowledge graph. Crawler technology is used to obtain 600 entity data, and the reliability of the proposed knowledge graph construction method is proved through experiments. Comparison reveals that the average value of the degree of Lingnan landscape painting is 0.034 higher than that of Western landscape painting, and the difference between the point-in degree and the point-out degree is 0.003 higher than that of Western landscape painting, which is not only an important intermediary and integration node, but also an active participant in cross-cultural interaction of techniques in the technique transmission network. Western landscape painting, on the other hand, reflects more of the systemic and endogenous nature of technique inheritance, with a relatively low density of cross-cultural integration interactions.*

KEYWORDS: *Lingnan landscape painting; Western landscape painting; multimodal knowledge graph; EIEA model; ERNIE model; technique inheritance*

1 Introduction

The Lingnan School of Painting was an emerging painting school that was active in the Guangdong region throughout Chinese history. It rose to prominence around the time of the Xinhai Revolution in China and, from its very beginning, embodied the spirit of cultural innovation in Guangdong [1]. Lingnan School of Painting is a famous school of painting at the beginning of the twentieth century, together with Beijing-Tianjin School of Painting and Maritime School of Painting, known as the three major regional schools of painting in the first half of the twentieth century in China, which boldly revolutionized the Chinese literati paintings for the purpose of advocating the "fusion of the ancient and the modern, and eclecticism between the East and the West" [2]. Lingnan landscape paintings have a wide range of subjects, emphasis on sketching, often with bias, medium brush, not confined to the ancient method, the use of color thick and colorful, reference to China and the West [3]. The national spirit and identity conveyed by the School of Painting have created a great driving force for cultural

*wuhuashi2000@163.com
https://doi.org/10.65102/is2026283
Published: 30 April, 2026

change in modern China. 21st century, the mutual exchange and collision of Eastern and Western cultures became more and more frequent, and Eastern and Western art absorbed and borrowed from each other, which provided the conditions for Western oil paintings to take root and grow in China. Accompanied by the progress of science and technology, human culture and national traditions as well as the way of life of human beings have undergone significant changes. However, looking at the history of the development of fine arts, we can see that pluralism is still its basic form of existence, and continuous innovation in response to the renewal of the times is the basic premise of its existence [4, 5].

The world culture is mainly divided into two major cultural patterns: East and West, and the study and comparison of the traditional cultures of the East and the West has a positive significance in promoting the harmonious development of today's world culture [6]. As an important part of national culture, the art of painting is eclectic, integrating human spirit, emotion and mind with great inclusiveness, and combining cultures of many disciplines with great integration, so it can be said that art is a universal language, which can make different cultures and different disciplines understand and appreciate each other [7-9]. From the perspective of landscape painting, both modern Lingnan landscape paintings in China and Western landscape paintings reflect the deep desire of people in both the East and the West to return to nature and embrace the inner world of nature [10-12]. Therefore, by comparing the techniques of modern Lingnan landscape paintings and Western landscape paintings, on the basis of understanding the development and evolution of Eastern and Western art [13-15], and by digging into the rich spiritual connotation, profound philosophical origins, and the influence of different national cultures in Eastern and Western painting techniques, we can have both theoretical guiding value and practical reference significance for the inheritance and innovation of contemporary Chinese painting techniques [16]. It has both theoretical guiding value and practical reference significance for the inheritance and innovation of contemporary Chinese painting techniques.

In this paper, we firstly specify the acquisition method of multimodal attribute data based on the dimension of painting works. A new model, EIEA, is proposed to solve the multimodal entity alignment task. Design the multimodal knowledge embedding module to extract the graph structure, relationships, attributes and visual features of entities. Develop EER module to improve the characterization of entities. Construct ERNIE pre-training model to realize joint relation extraction and knowledge fusion in combination with pointer network. Self-construct datasets of modern Lingnan landscape paintings and Western landscape paintings, introduce different percentages of noise to evaluate the stability of the EIEA model. Verify the validity of ERNIE model through comparative experiments. Take technique inheritance as the central knowledge point and establish a knowledge map. Relying on the results of point-centeredness comparative analysis, analyze the differences between the technique inheritance patterns of Lingnan landscape painting and Western landscape painting.

2 Painting-oriented knowledge graph construction method for multimodal attribute information

2.1 Data acquisition

The main task of data acquisition is to complete the collection of data information on paintings and authors, and the data sources include Baidu Encyclopedia, Wikipedia, Google Scholar and other aspects. However, the knowledge data acquired from the network is mostly some semi-structured data, the form does not fit the structure of the strong correlation of the data table in

the relational database, but contains the structure of the label or data field that separates the semantic elements. Therefore, this paper adopts crawler technology for data crawling, and carries out certain processing on the acquired unstructured data, in order to prepare for the subsequent extraction of entities and entity relationships to form a knowledge graph.

Crawling the corresponding data from the website needs to use the parsing technology, this paper data parsing using BeautifulSoup technology to the DOM tree parsing, for example, using the following way to a knowledge node to obtain.

Soup = BeautifulSoup (html_doc, 'lxml');

Soup.find_all (re.compile ("^b"));

Beautiful Soup technology mainly uses the characteristics of structured labels of DOM trees to extract labels by searching according to node name, attribute search, node text search, etc., and finally serialize them to local disk.

The data obtained by using web crawler can not be used as a data source for entity as well as relationship extraction due to its confusion, so it is necessary to clean the data, i.e., eliminate the data that does not meet the criteria, categorize the type of data it belongs to, and so on. Finally, after a series of operations, a clean data source is obtained, and the next operation to be done is the extraction of entities and relationships.

2.2 Multimodal Entity Alignment Models

2.2.1 Multimodal Knowledge Graph Embedding

This paper presents a new model, Enhanced Entity Interaction Modeling for Multimodal Entity Alignment (EIEA). In multimodal knowledge graphs, an entity is often described by various features of multiple modalities (or views), i.e., graph structures, relationships, attributes, and visual information, which complement each other. In this section, EIEA learns the feature representations of different modalities using separate encoders appropriate to the nature of the signal. Theoretically, EIEA can support more modalities such as entity name and entity description information.

(1) Graph structure embedding

In multimodal knowledge graphs, equivalent entities tend to have similar neighbor nodes, i.e., they share similar structural information. To capture the structural information of entities and discover potentially aligned entities, MMKE uses a graph attention network (GAT) to aggregate the structural information of nodes from the neighbors of entities. Formally, a homogeneous graph $\mathcal{G}=(\mathcal{V},\mathcal{E})$ is first constructed on the basis of the set of relational triples T_r. Specifically, each node $\mathcal{V}_i \in \mathcal{V}$ represents an entity e_i, and if there exists a ternary (e_i, r_k, e_j) belonging to T_r, then two edges are added to $\mathcal{E}$: $(\mathcal{V}_i, \mathcal{V}_j)$ and $(\mathcal{V}_j, \mathcal{V}_i)$. Then, given an entity e_i, this section generates its set of one-hop neighbors $\mathcal{N}_i$ based on $\mathcal{G}$ via self-loops. For each entity e_i, its neighbor aggregation process is defined as follows:

$$h_i^g = \mathrm{Re}\,LU\left(\sum_{j\in\mathcal{N}_i} \alpha_{ij} h_j^g\right) \tag{1}$$

where $h_i^g, h_j^g \in \mathbb{R}^d$ is the hidden state of entities e_i and e_j, d is the dimension of the hidden layer, and $\mathrm{Re}\,LU(\cdot)$ denotes that it is necessary to perform ReLU nonlinear operations, and α_{ij} is the importance of entity e_j to entity e_i, denoted as follows:

$$\alpha_{ij} = \frac{\exp\left(Leaky\,\mathrm{Re}\,LU\left(a^{\top}[Wh_i^g \oplus Wh_j^g]\right)\right)}{\sum_{u\in\mathcal{N}_i}\exp\left(Leaky\,\mathrm{Re}\,LU\left(a^{\top}[Wh_i^g \oplus Wh_u^g]\right)\right)} \tag{2}$$

where $W \in \mathbb{R}^{d\times d}$ denotes a diagonal weight matrix that reduces the computational effort, $a \in \mathbb{R}^{2d}$ is a learned weight parameter, $\oplus$ denotes the column concatenation operation, and $Leaky\,\mathrm{Re}\,LU(\cdot)$ denotes the need for the LeakyReLU nonlinear operation. In order to stabilize the self-attentive learning process, EIEA performs $K=2$ heads of parallel independent attention in Eq. (1), and finally connects these features in order to obtain a graph-structured embedding h_i^g of the entity e_i:

$$h_i^g = \mathop{\Big\|}_{k=1}^{K}\mathrm{Re}\,LU\left(\sum_{j\in\mathcal{N}_i}\alpha_{ij}^k h_j^g\right) \tag{3}$$

where α_{ij}^k is the normalized attention coefficient calculated for the k th attention.

(2) Relationship and attribute embedding

Since aligned entities usually have similar types of relations and attributes, modeling the knowledge of these two modalities will help entity alignment. Therefore, EIEA treats the relationships and attributes of entities as bag-of-words features and feeds them into a feed-forward layer to explicitly model these two modalities. In order not to lose generality, EIEA considers only the top $l(l=1000)$ most frequent relations and attributes. For the entity e_i in the entity set E with the set of relations $\{r_1, r_2, \cdots, r_l\}$ and the set of attributes $\{a_1, a_2, \cdots, a_l\}$, EIEA constructs the count-based x-hot vector $f_i^r, f_i^a \in \mathbb{R}^{1\times l}$ to represent relationship and attribute features, respectively. Where the j th element of the vector f_i^r (or f_i^a) is the count x of the j th relation (or attribute) of the corresponding entity e_i. The relation embedding h_i^r and attribute embedding h_i^a of the entity are computed as follows:

$$h_i^m = W_m f_i^m + b_m, m \in \{r, a\} \tag{4}$$

where W_m, b_m denote the weight matrix and Bayesian bias of modality m.

(3) Visual embedding

Visual knowledge can reflect some entity characteristics more intuitively than other modal knowledge. Usually, entities with the same concept in the real world have more similarity in visual features. Therefore, visual knowledge improves the alignment to some extent. In this section, EIEA employs pre-trained visual models (PVMs) such as VGG16, DenseNet and TimeSformer to learn image and video embeddings. Specifically, EIEA inputs the image p_i of the entity e_i into VGG16; similarly, for the video v_i of the entity e_i, keyframes are first sampled for the video, which is then input into TimeSformer. The output before the last fully connected layer is taken and linearly transformed to obtain the image embedding h_i^p of the entity and the video embedding h_i^v:

$$h_i^m = W_m PVM\left(m_i\right) + b_m, m \in \left\{p, v\right\} \tag{5}$$

2.2.2 Enhanced entity representation

After obtaining a set of multimodal feature embeddings $\left\{h^g, h^r, h^a, h^p, h^v\right\}$ (where h^g is the matrix, and each row denotes the entity embeddings learned from the graph structure), this paper proposes the Enhanced Entity Representation (EER) module to obtain entity embeddings with more representational power, including two components: hybrid block attention (MBA) and multimodal fusion (MMF).

(1) Mixed Block Attention (MBA)

Exploring pairwise interactions between any pair of entities in each modality (especially between an entity and its neighboring entities) is crucial. Based on this insight, EIEA developed the Mixed Block Attention (MBA) component, inspired by Graph Transformer and FLASH. This component efficiently models the neighborhood and context information of entities and mines pairwise entity node interactions to enhance entity representations.MBA consists of two phases: local block self-attention and global attention across blocks, and its implementation is shown below.

Before delving into the details of MBA, the following preparatory notes must be provided in this section. In order to efficiently solve the above tasks and exploit the parallel processing capabilities of the Transformer-based model, this section employs the following strategy to sort the entities in the set of entities and to bring each entity closer to its neighbors before modular multimodal knowledge embedding (MMKE). The details are as follows, given a multimodal knowledge graph $KG=\left(E,R,A,P,V,T_r\right)$, this section assumes that E contains N entities. N_i is the set of single-hop neighbors of entities numbered ID_i. Specifically, an entity, numbered ID_1, is first randomly selected from E. Then, the entities in N_1 are numbered starting from ID_2. Next, the operation is repeated for all remaining entities in E according to $\{N_2, N_3, \cdots\}$. It is worth noting that if an entity has been numbered in N_i, it cannot be numbered again in $N_j\left(i<j\right)$. Finally, the entity encoding set $ID=\left\{ID_1,\cdots,ID_N\right\}$ is obtained, where the embedding of the entity numbered ID_i is the i th element in h, and $h\in\left\{h^g, h^r, h^a, h^p, h^v\right\}$ denotes the embedding matrix learned from some type of modal information.

For a unimodal embedding matrix h, the MBA first divides it into B non-overlapping blocks with a given size c, where the value of c is determined by the statistical distribution of the entity's neighborhood size. Then, for the ith block $h_{(i)}\subset h$, an affine transformation (i.e., a linear mapping of the activation function) is applied to it to obtain $U_{(i)}$, $X_{(i)}$, and $Z_{(i)}$:

$$U_{(i)}=\phi_u\left(h_{(i)}W_u\right),\ X_{(i)}=\phi_x\left(h_{(i)}W_x\right)\in\mathbb{R}^{c\times t} \tag{6}$$

$$Z_{(i)}=\phi_z\left(h_{(i)}W_z\right)\in\mathbb{R}^{c\times s} \tag{7}$$

where W_u, W_x, W_z are trainable dense matrices, t denotes the intermediate dimension of the expansion, s is the dimension of the hidden layer, and $\phi\left(\cdot\right)$ is the element-by-element activation function. Finally, four types of attention heads $Q_{(i)}^{quad}$, $K_{(i)}^{quad}$, $Q_{(i)}^{lin}$, and $K_{(i)}^{lin}$ are generated from $Z_{(i)}$ by applying per-dim scaling and biasing. Based on these four attention

heads, two stages, local block self-attention and global attention across blocks, are designed in this section.

Local block self-attention. This stage is designed to capture short-range interactions between entities, i.e., interactions between entities and their neighbors. Local secondary attention is independently introduced into each block as a head, which is formulated as follows:

$$X_{(i)}^{quad} = \frac{1}{cs}\mathrm{Re}LU^2\left(Q_{(i)}^{quad}K_{(i)}^{quad\top}\right)X_{(i)} \tag{8}$$

where $X_{(i)}^{quad}$ is the output of the local block self-attention phase. This formulation realizes multi-head attention with B heads (i.e., each block is a head) and block size c, highlighting the close interaction of entities within a block and the efficiency of the computational process.

Global attention across blocks. This stage considers sparse, remote interactions between entities across different blocks. In detail, this section introduces a global linear attention mechanism that can efficiently handle long sequences and reduce the complexity to linear, as shown in FLASH and Linformer. Based on the global linear attention mechanism, the phase is formulated as follows:

$$X_{(i)}^{lin} = \frac{1}{n}Q_{(i)}^{lin}\left(\sum\nolimits_{j=1}^{B}K_{(j)}^{lin\top}X_{(j)}\right) \tag{9}$$

where $X_{(i)}^{lin}$ is the output of the global attention phase across blocks. Subsequently, $X_{(i)}^{quad}$ and $X_{(i)}^{lin}$ are firstly summed up and fed into the gated attention unit (GAU) to obtain the output of the ith block $h_{(i)}$:

$$h_{(i)} = \left(U_{(i)} \odot \left(X_{(i)}^{quad} + X_{(i)}^{lin}\right)\right)W \tag{10}$$

The presence of gating permits the use of simpler/weaker attention machines than the multi-head self-attention without mass loss. After obtaining the B -block output $\left\{\hat{h}_{(1)},\cdots,\hat{h}_{(i)},\cdots,\hat{h}_{(B)}\right\}$, the MBA utilizes the row-connection operation $\|$ and the adaptive weighting remote residual join to obtain the final augmented entity representation h:

$$h = w_1\left(h_{(i)}\right)\Big\|_{i=1}^{B} + w_2 h \tag{11}$$

where w_1 and w_2 are trainable weight parameters. Note that since the MBA is implemented in each modality, ultimately this section obtains a set of augmented entity representations $F = \left\{h^g, h^r, h^a, h^p, h^v\right\}$

(2) Multimodal Fusion (MMF)

In order to facilitate effective multimodal embedding fusion, this chapter designs a multimodal fusion (MMF) component based on a weighting mechanism and enhanced entity representations. Specifically, given a multimodal knowledge graph corresponding to

$F = \left\{ h^g, h^r, h^a, h^p, h^v \right\}$ of the multimodal knowledge graph, MMF first performs L2 normalization on the augmented entity representations of each modality in F, and then obtains the joint embedding h_i^{join} via a trainable weighted connection, i.e:

$$h_i^{join} = \bigoplus_{m \in \{g,r,a,p,v\}} \left[\frac{\exp(w_m)}{\sum_{j \in M} \exp(w_j)} h_i^m \right] \tag{12}$$

where w_m is the trainable weight of modality m. However, the current joint embedding is coarse-grained with no interaction between modalities.

2.3 Multimodal Knowledge Graph Construction

2.3.1 ERNIE-based Joint Extraction Modeling

Knowledge extraction is an important part of constructing knowledge graph, this section proposes an entity-relationship joint extraction model incorporating ERNIE pre-training model combined with pointer network under the framework of cue learning, which consists of two parts, and the structure of the model is shown in Fig. 1, which are the encoding layer and ternary extraction layer, respectively, and the use of the knowledge joint extraction model in the knowledge extraction process will be described in this section.

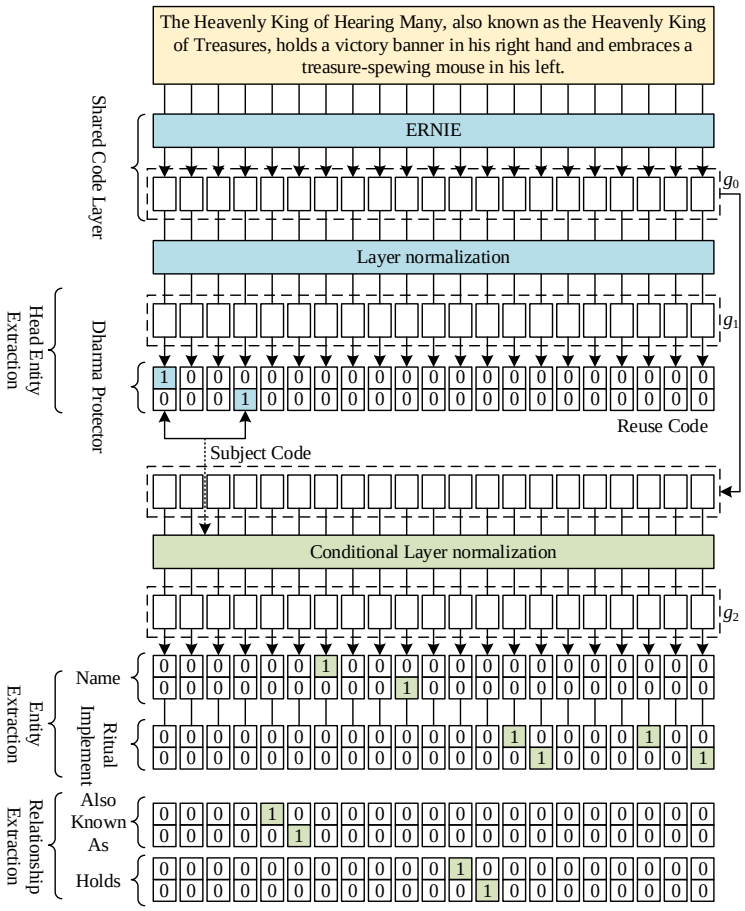

Figure 1: Joint extraction model based on pointer network

(1) ERNIE pre-trained model coding layer

The joint extraction model includes two parts: the shared coding layer and the ternary extraction layer, in which the ternary extraction layer includes three parts: head entity extraction, entity extraction, and relation extraction.

The process of ERNIE model as a coding layer in the extraction task of multimodal Tangka knowledge graph is divided into three steps: 1) Introducing ERNIE as an encoder through the word embedding layer, inputting the input sentence into the ERNIE layer, and obtaining the feature vectors of each character; 2) Modeling the ternary in the ternary extraction layer, extracting the head entity using the sentence encoding and, according to the relationship category, extracting the tail entity; 3) Construct the downstream pointer network and decode the ternary.

Using the output sequence of ERNIE model $g_0 = (g_1, g_2, \cdots, g_n)$ to extract the SUBJECTS, followed by the OBJECT corresponding to the SUBJECTS according to the category, and finally build the cascade structure and decode it using the pointer network Output ternary. Extract the head entity: normalize the sentence code g_0 to get the sentence code g_1, use g_1 to calculate each token in the input sentence, predict the probability that it is the start of $\left(q_i^{s\_start}\right)$ or the end of $\left(q_i^{s\_end}\right)$, and label the token with "0" and "0" for each token. token labeled "0/1", set a threshold and determine whether it is greater than the threshold according to the probability (greater than the threshold token labeled as 1, and vice versa as 0). The calculation method is shown in Equation (13) and Equation (14).

$$q_i^{s\_start} = \delta\left(\omega^{s\_start} g_1^i + a^{s\_start}\right) \tag{13}$$

$$q_i^{s\_end} = \delta\left(\omega^{s\_end} g_1^i + a^{s\_start}\right) \tag{14}$$

The encoding of the head entity and the sentence encoding g_0 are feature fused to obtain a new sentence encoding g_2, and the new sentence encoding g_2 is utilized to compute for each token in the sentence in the j th SUBJECT and n th RELATIONSHIP CONDITION, the OBJECT is the beginning $\left(q_{i,j,n}^{s\_start}\right)$ and ending $\left(q_{i,j,n}^{s\_end}\right)$ probabilities, as above. As shown in Eqs. (15) and (16).

$$q_i^{o\_start} = \delta\left(\omega^{o\_start} g_1^i + a^{o\_start}\right) \tag{15}$$

$$q_i^{o\_end} = \delta\left(\omega^{o\_end} g_1^i + a^{o\_start}\right) \tag{16}$$

where $\omega^{(\cdot)}$ denotes the trainable weights, $a^{(\cdot)}$ denotes the trainable bias, δ denotes the sigmoid activation function, and g_1 is the sentence code.

(2) Language model masking strategy based on cue learning

The cue learning framework is introduced to give the model a cue template through the accompanying input, which is used to guide the downstream task operation. The text generation ability of the language model is stimulated, thus improving the model efficiency. Before performing knowledge extraction, the cue template is specified for pre-training based on the task to be extracted. The traditional BERT model is similar in structure to ERNIE, which is composed of Embedding layer and Transformer layer, although it considers the contextual

semantics but not the lexical and syntactic features, resulting in the model's poor ability for understanding the contextual relations of long sequences, so in order to improve the model's ability to generalize the sentences and represent the features, the ERNIE adopts an improved MLM strategy, which masks a character in a sentence with [MASK], and then uses the model to predict the actual character of the masked word, and improves the original method of [MASK] Chinese characters to [MASK] Chinese words, and adds some lexical information into the model to enhance the model representations. The difference between the BERT model and the ERNIE model in the MLM task example is shown in Figure 2. As shown in Fig. 2. The use of cue learning is based on discrete prompts, no parameter references, fixing the pre-trained model to do the [MASK] task, which solves the problem of underfitting of traditional binary classification models for small sample problems, and vocab θ is a pre-set candidate set of entity phrases.

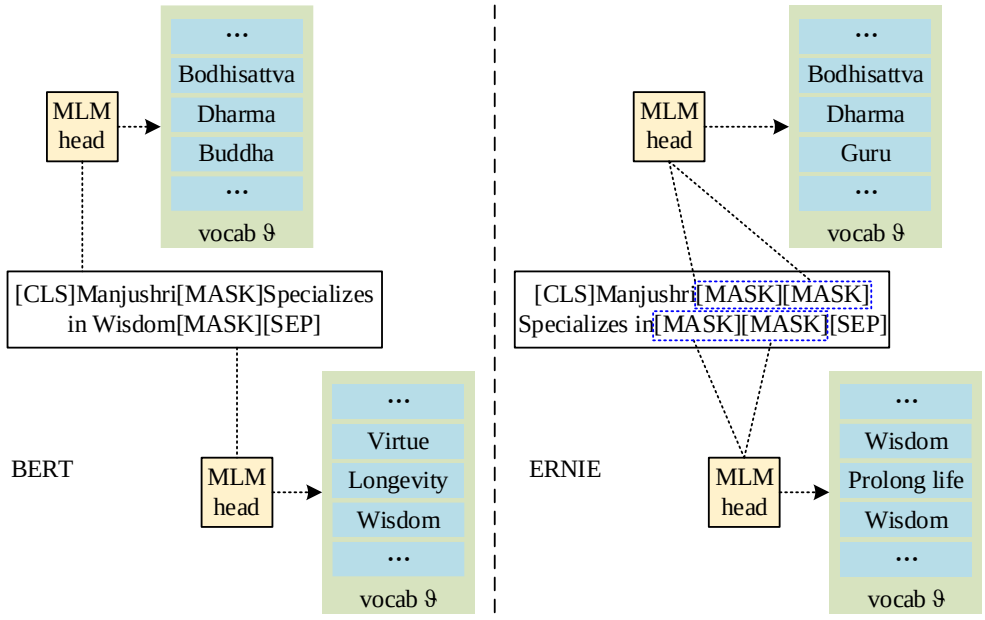

Figure 2: Example MLM of BERT model and ERNIR model

2.3.2 Knowledge integration

Due to the dispersed data from a wide range of sources and the different representations of the same objective entity in different works, it is necessary to integrate and correlate data under a unified specification for the acquired knowledge. In this section, different semantic representations of the same entity in different writings are correlated so as to solve multiple semantic disambiguation of the same entity. A set is formed according to the predefined entities and relationship words, and the word frequency of each word in the set is calculated to generate the word frequency vector. Based on the ERNIE pre-trained language model and the cosine similarity formula, the cosine similarity of different entity vectors is calculated, as shown in Equation (17).

$$similarity = \cos(\theta) = \frac{A * B}{\|A\| * \|B\|} = \frac{\sum_{i=1}^{n} A_i \times B_i}{\sqrt{\sum_{i=0}^{n} (A_i)^2} \times \sqrt{\sum_{i=1}^{n} (B_i)^2}} \tag{17}$$

where A, B denote the word frequency vectors of different entities, A_i and B_i denote the word frequency components of A, B. The result of similarity is compared with 1 and 0. If the calculated value is closer to 1, it means that the two entities are more similar and can be fused with a unified entity name; if the calculated value is closer to 0, it means that the similarity of the two entities is extremely low, and their corresponding entities are retained. The knowledge fusion process is shown in Fig. 3, which generates word frequency vectors through word frequency statistics, and after the calculation of ERNIE representation and cosine similarity, which results in the threshold value converging to 1 and possessing a high degree of similarity, the two representations are considered to be the same entity, and the entity name is unified.

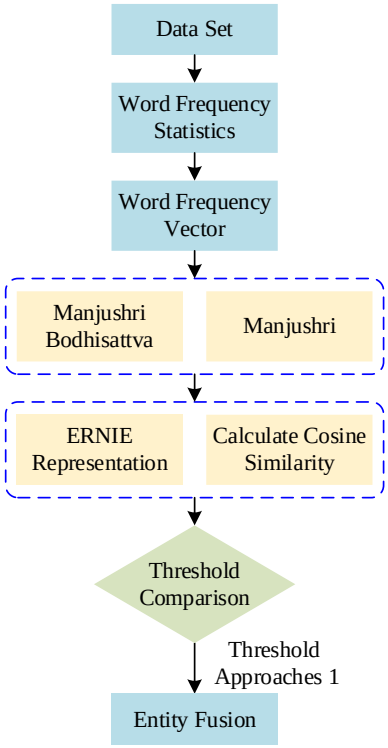

Figure 3: Knowledge fusion process

3 Analysis of Modern Lingnan Landscape Painting and Western Landscape Painting Techniques Based on Knowledge Mapping

This paper uses crawler technology to obtain the data of modern Lingnan landscape paintings and Western landscape paintings from museums, art galleries digital resources, academic papers and professional databases. According to the entity category division this paper extracts three main entity categories: author, work, technique. In the end, a total of 600 entities are obtained, including 60 author entities, 360 work entities and 180 technique entities, including text and image modalities.

3.1 Entity alignment

Five datasets are constructed by introducing different percentages of noise, and five experiments are conducted on each dataset to evaluate the performance of the algorithm with

three indexes: recall, accuracy and F-value. The specific experimental results are shown in Table 1, the first column indicates the number of entities contained in the dataset, the number of correctly aligned entities indicates the number of manually labeled 200 sets of entity groups successfully aligned after algorithmic computation, and the author, work and technique entities indicate the number of different types of entities successfully matched after algorithmic alignment. The last three columns are the total recall, accuracy and F-measure metrics for the three types of entities. The changes in the average metrics of the five experiments with different noise matching data are shown in Fig. 4. With the introduction of different amounts of noise, the successful pairing accuracy of all three categories of entities shows a decreasing trend. The algorithm in this paper achieves an average accuracy of 85.9% in five experiments without the introduction of noise, and the highest can reach 89.9%. The experimental results show that although the accuracy rate and F-measure show a significant decreasing trend as the percentage of introduced noise increases, the accuracy rate is still above 65% and the F-measure is above 70%, and the recall rate is not sensitive to the addition of noise.

Table 1: Changes in evaluation indicators under the influence of noise

The number of entities	Align the correct quantity	Author entity	Work entity	Technique entity	Recall	Precision	F-measure
600+0%noise	153	16	98	39	0.843	0.847	0.845
	153	9	91	53	0.849	0.852	0.850
	152	14	104	34	0.847	0.831	0.839
	156	12	95	49	0.862	0.868	0.865
	158	15	101	42	0.894	0.899	0.896
600+20%noise	151	12	88	51	0.833	0.797	0.815
	162	14	103	45	0.859	0.814	0.836
	148	16	91	41	0.804	0.772	0.788
	157	13	87	57	0.865	0.823	0.843
	149	9	86	54	0.799	0.765	0.782
600+40%noise	153	11	102	40	0.844	0.765	0.803
	147	14	103	30	0.791	0.723	0.755
	154	15	95	44	0.842	0.762	0.800
	158	17	98	43	0.865	0.781	0.821
	146	8	101	37	0.834	0.745	0.787
600+60%noise	151	16	89	46	0.841	0.723	0.778
	155	21	96	38	0.853	0.741	0.793
	154	19	92	43	0.864	0.755	0.806
	158	15	103	40	0.835	0.702	0.763
	152	13	100	39	0.871	0.773	0.819
600+80%noise	156	22	96	38	0.823	0.708	0.761
	161	18	100	43	0.847	0.745	0.793
	153	14	92	47	0.831	0.711	0.766
	159	9	98	52	0.883	0.722	0.794
	155	17	91	47	0.852	0.746	0.795
600+100%noise	166	13	96	57	0.856	0.732	0.789
	151	16	89	46	0.861	0.713	0.780
	155	14	100	41	0.854	0.678	0.756
	154	12	91	51	0.839	0.657	0.737
	155	14	94	47	0.855	0.702	0.771

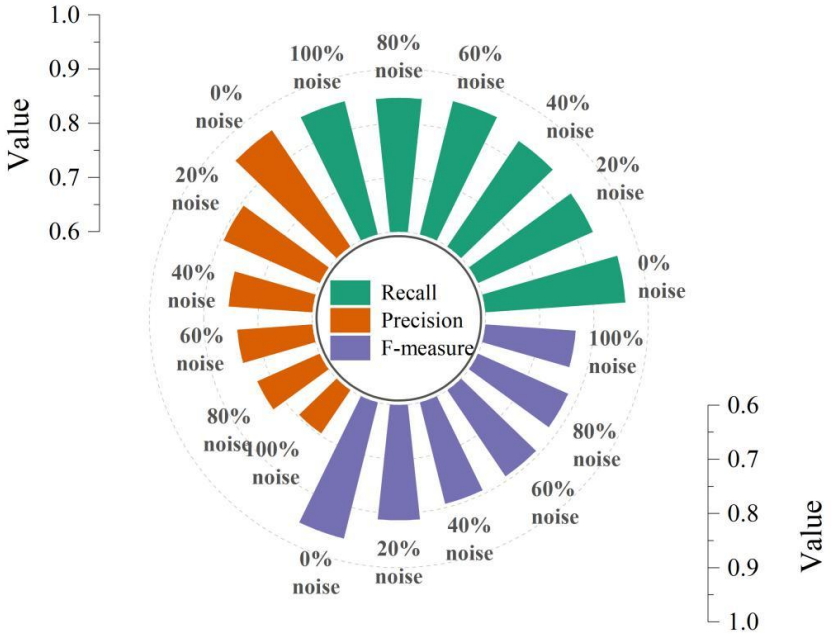

Figure 4: Average index changes of five experiments

3.2 Relationship Extraction

Bert+BILSTM and BERT+MLP are selected as the control models for the relationship extraction experiments, and the comparison results of the PRC curves of different models are shown in Figure 5. In the interval of recall 0~0.5, there is no significant difference in the performance of the three models. In the recall interval of 0.05~0.25, the ERNIE model proposed in this paper performs significantly better than the control model. The model in this paper applies the existing knowledge and model parameters to the new task through the method of transfer learning, which realizes the joint extraction of knowledge to a certain extent, and is obviously better than the streaming extraction method.

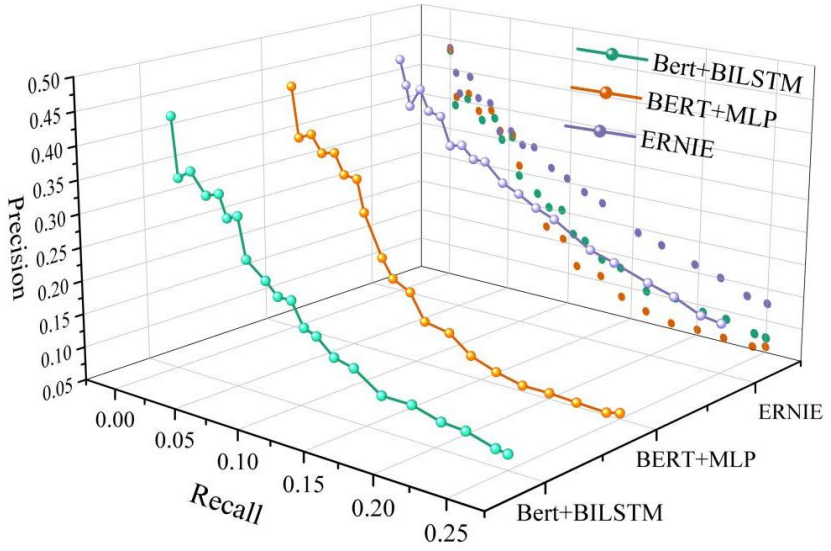

Figure 5: Comparison results of PRC curves for different models

3.3 Knowledge map construction

The results of partial knowledge association radiating around the center knowledge point of technique inheritance are shown in Table 2, which contains techniques (numbered T1~T180), knowledge association weights, authors (numbered A1~A60), and works (numbered W1~W360). The knowledge association mainly introduces the degree of closeness between different techniques, such as the knowledge association weight of some techniques reaches 0.9, which lays the foundation for further construction of a complete knowledge graph.

Table 2: Partial results of knowledge association

	Technique A	Technique B	Knowledge correlation weight	Author	Work
1	T1	T5	0.7	A3	W2
2	T38	T12	0.9	A7	W15
3	T3	T66	0.6	A11	W24
4	T26	T9	0.6	A4	W21
5	T15	T23	0.9	A52	W133
6	T24	T7	0.8	A12	W78
7	T9	T44	0.5	A4	W9
...	...	...	...	...	...

Further subgraph approximation is performed on the captured individual knowledge subgraphs. Subgraph approximation is to process the original knowledge graph and remove redundant knowledge subgraphs while keeping the original knowledge graph system unchanged. Experiments are conducted on different knowledge point weight ratios and knowledge association weight ratios to determine the optimal threshold, and the results of threshold selection are shown in Figure 6. The selection of threshold λ (including knowledge weight ratio and knowledge association weight ratio) shows an overall negative correlation to the number of approximation diagrams, i.e., as the number of approximation diagrams becomes smaller, the computed values of knowledge point weight ratio and knowledge association weight ratio gradually become larger. When the number of simplification reaches 120, the knowledge point weight ratio and knowledge association weight ratio have tended to be unchanged, and at this time, the calculated value of the knowledge point weight ratio is between [0.46,0.48], and the value of the knowledge association weight ratio is between [0.46,0.51], and the final threshold value of λ=0.47 is taken to be the maximal simplification effect on the data of the original knowledge graph. In the process of simplification, the subgraphs whose knowledge point weight ratio or knowledge association weight ratio is less than 0.47 are deleted, and the invalid knowledge subgraphs are removed. Then the remaining knowledge subgraphs are subjected to similarity calculation to obtain a high-density set of knowledge subgraphs, which finally realizes the construction of two knowledge graphs of modern Lingnan landscape painting and Western landscape painting.

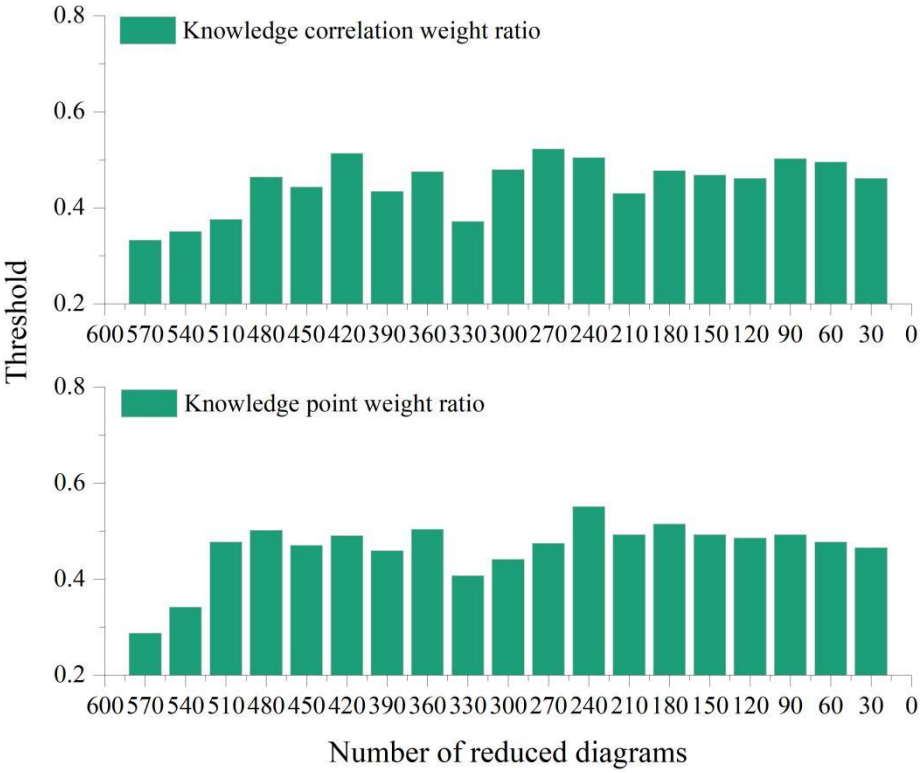

Figure 6: Threshold selection results

3.4 Comparative Analysis of Technique Inheritance

3.4.1 Point centrality analysis

Using UCINET 6.0 software to carry out the point degree centrality analysis, the visualization results of the point degree centrality analysis of the two genres of Lingnan landscape painting and Western landscape painting are shown in Figure 7 (a~b). Technique inheritance behavior, Lingnan landscape painting degree maximum value for and the minimum value of the gap is large, the difference is 31.139, the average value is 5.740, point into the degree of the maximum value of the difference between the minimum value of 3.624, point out of the degree of the maximum value of the difference between the minimum value of 3.439, the difference between the degree of the point into the degree of the gap between the degree of point and the degree of point out of the degree of the larger, and the heterogeneity of the network of 0.99%, tends to be close to 1, indicating that the entire network has a strong centralized trend, the It has a better effect on the behavior of technique transmission. The average value of the degree of Western landscape painting is 5.706, which is 0.034 lower than that of Lingnan landscape painting, indicating that the nodes of the relevant techniques of Lingnan landscape painting are in a more frequently interacting and associated position in its technique inheritance network. Meanwhile, the difference between the point-in degree and point-out degree of Western landscape painting is small, only 0.001, and the integration and bidirectional mobility of cross-cultural interaction of its technique inheritance is relatively weak.

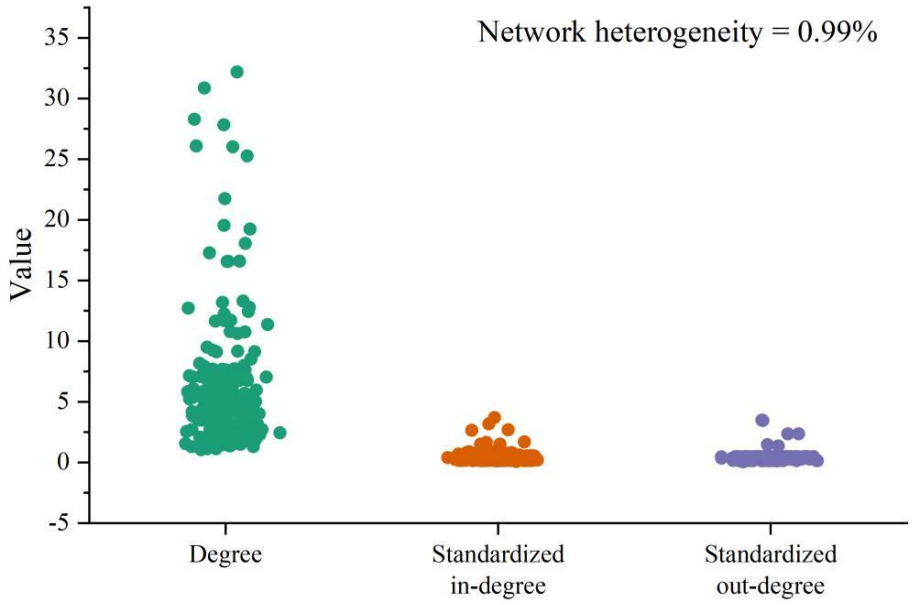

(a) Lingnan landscape painting

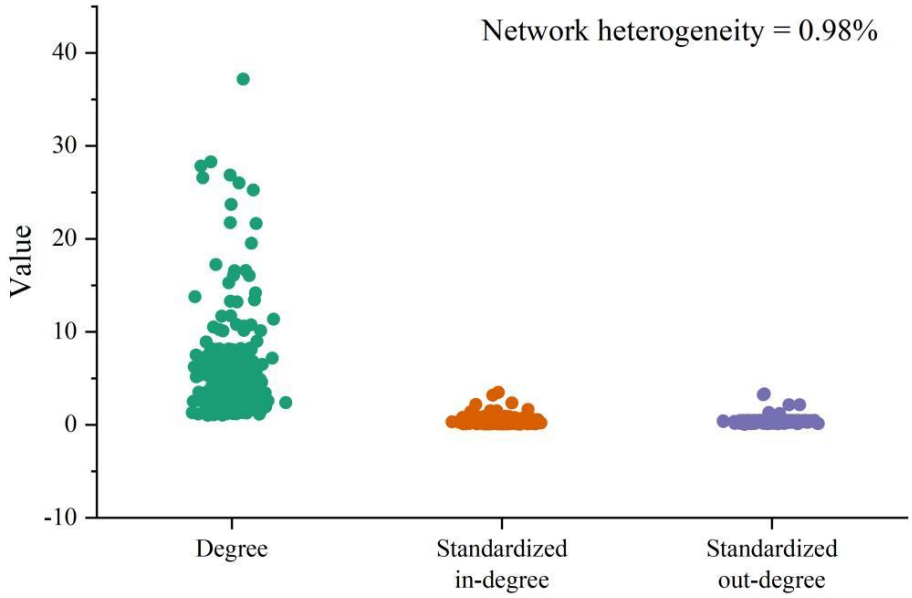

(b) Western landscape painting

Figure 7: Visualization results of point degree centrality analysis

3.4.2 Nodality index correlation analysis

In this part, Top N analysis will be carried out to calculate the correlation between nodes and the contribution of technique inheritance in segments, and the total contribution of nodes to technique inheritance, S(j), will be sorted, and the results of correlation between Lingnan landscape paintings and Western landscape paintings are shown in Table 3 and Table 4 respectively. Among them, the N value takes the 20th item as the first item, and then the N value is taken sequentially in an isotropic series with a tolerance of 20 until it is taken to 180 nodes. Combining Tables 3 and 4, it can be seen that the inheritance of techniques in small-scale social networks is suitable to be measured by point degree centrality. As the number of nodes increases, the network members continue to increase, the network size continues to

expand, the correlation coefficient gradually increases, showing a positive correlation.

Table 3: Correlation results of Lingnan landscape painting

Top N	Corr (Dg, s(j))	Corr (DI, s(j))	Corr (Bt, s(j))
20	0.075	0.064	0.136
40	0.142	0.123	0.191
60	0.191	0.168	0.213
80	0.235	0.197	0.246
100	0.282	0.235	0.272
120	0.332	0.267	0.308
140	0.369	0.278	0.324
160	0.391	0.322	0.359
180	0.435	0.339	0.372

Table 4: Correlation results of Western landscape painting

Top N	Corr (Dg, s(j))	Corr (DI, s(j))	Corr (Bt, s(j))
20	0.059	0.054	0.119
40	0.127	0.103	0.164
60	0.184	0.145	0.183
80	0.213	0.172	0.216
100	0.266	0.204	0.255
120	0.305	0.235	0.278
140	0.343	0.258	0.303
160	0.375	0.287	0.314
180	0.406	0.309	0.326

4 Conclusion

In this paper, EIEA and ERNIE models are constructed to carry out a comparative analysis using the proposed methods for the differences in the inheritance of techniques between modern Lingnan landscape painting and western landscape painting.

(1) The average accuracy, recall, and F-value of EIEA model still reach 85.3%, 69.6%, and 76.7%% respectively under the introduction of 100% noise, which has a better effect on entity matching. The relative trends of the three relational extraction models are basically the same in the interval of recall 0~0.5. In the recall rate 0.05~0.25 interval, the accuracy of ERNIE model is much higher than the control model.

(2) The analysis of point degree centrality shows that in the behavior of technique inheritance, the average value of Lingnan landscape painting degree is 5.740, which is 0.034 higher than that of Western landscape painting, reflecting that the Lingnan School of Painting shows stronger network centrality in the process of technique inheritance. The difference between the point-in degree and point-out degree of Lingnan landscape painting is 0.003 larger than that of Western landscape painting, showing that the Lingnan School of Painting has both absorbed a large number of foreign techniques and actively combined these elements with local traditional techniques and further spread them outward or influenced the development of other techniques.The results of the Top N analysis proved the validity of the centrality of the point-degree measure.

Funding

This research was supported by the Guangdong Provincial Philosophy and Social Sciences Planning 2024 Annual Lingnan Culture Project: "A Study on the Mutual Relationship between Modern Lingnan Landscape Painting and Overseas Landscape Painting" (Approval Number: GD24LN17).

References

[1] Ho, R., Vollmer, S. H., & Zheng, X. (2024, July). Subverting Syntax: Experimental narratives from the Post-Lingnan School of Painting. In Proceedings of EVA London 2024 (pp. 85-93). BCS Learning & Development.

[2] Liu, Y. (2019). Art for the New Nation: The Rise of the Lingnan School in the 1920s and the 1930s. HKU Theses Online (HKUTO).

[3] Lingbin, K. (2016). The Correction of the Proof-read Edition of the Legend of the Painters of Lingnan Painting School. Libraly Journal, 35(9), 107.

[4] Zhang, P., Chen, H., & Zhou, S. (2022). Brief History of Painting in Modern China. Cultural and religious studies, 10(5), 236-241.

[5] Chen, C., & Zuo, J. (2018, December). The Symmetrical Beauty and Its Cultural Connotation of Lingnan Architecture. In 2018 International Conference on Management, Economics, Education, Arts and Humanities (MEEAH 2018) (pp. 143-149). Atlantis Press.

[6] Pae, H. K. (2020). The east and the west. Script effects as the hidden drive of the mind, cognition, and culture, 107-134.

[7] Yang, T., Silveira, S., Formuli, A., Paolini, M., Pöppel, E., Sander, T., & Bao, Y. (2019). Aesthetic experiences across cultures: Neural correlates when viewing traditional Eastern or Western landscape paintings. Frontiers in psychology, 10, 798.

[8] Liu, W. (2021). Analysis on the Collision and Fusion of Eastern and Western Paintings in the Context of Globalization. Thought, 7(8).

[9] Trawiński, T., Zang, C., Liversedge, S. P., Ge, Y., Fu, Y., & Donnelly, N. (2024). The influence of culture on the viewing of Western and East Asian paintings. Psychology of Aesthetics, Creativity, and the Arts, 18(2), 121.

[10] Kye, Y. H. (2014). The spirit of the age in mathematics and art: The Eastern and Western perspective painting. Journal of Mathematics and System Science, 4(1), 56.

[11] Duan, X. (2023). A study of Chinese and Western landscape painting from the comparative perspective. Frontiers in Art Research, 5(13), 1-7.

[12] Shen, H. (2024). Exploring the Heterogeneity and Commonality of Emotional Expression in Eastern and Western Painting Art. Journal of Humanities, Arts and Social Science, 8(8).

[13] Jin, J. (2025). The Teaching Reform and Practice of Chinese Gongbi Painting Based on Lingnan Local Culture. Lecture Notes in Education, Arts, Management and Social Science, 3(6), 285-290.

[14] Zhang, H. (2024). A comparative study on the painting forms of western oil painting and Chinese ink painting. American Journal of Arts and Human Science, 3(2), 39-45.

[15] Yu, X. (2025). The Transcendence of Traditional Concepts in Modern Chinese and Western Painting. Literature, Language and Cultural Studies, 1(3), 33-43.

[16] Sun, J., & Xiao, C. (2008). An Analysis on the Influence of Line in Chinese And Western Painting on Visual Shaping Language. Asian Social Science.